Assessment of the Atmospheric Extinction for Solar Tower Power Plants along the Sun Belt: Preliminary Results

Aitor Marzo[1], Aloïs Salmon[2], Jesús Polo[3], Jesús Ballestrín[4], Joaquín Alonso-Montesinos[5] and Diego Pulido[1]

[1] Centro de Desarrollo Energético Antofagasta, University of Antofagasta, Antofagasta (Chile)

[2] Fraunhofer Chile Research, Center for Solar Energy Technologies, Santiago (Chile)

[3] Photovoltaic Solar Energy Unit, Renewable Energy Division CIEMAT, Madrid (Spain)

[4] CIEMAT-Plataforma Solar de Almería. Point Focus Solar Thermal Technologies Unit, Almería (Spain)

[5] Chemistry and Physics Department, University of Almería, Almería (Spain)

Abstract

Atmospheric extinction between heliostats and receivers has become an important issue in recent years as it limits the amount of useful local solar resource available in large solar power tower plants. Therefore, considering only direct normal solar irradiation in the solar resource assessment for solar power tower plant projects is inadequate and conducts to errors. In this paper, we present preliminary results of the evaluation of heliostat-to-tower atmospheric extinction values along the Sun Belt. The results show that the Atacama Desert in Chile has the lowest values of atmospheric extinction for a 1 km slant range, at around 4%. In general, it is in West Africa, Arabian Peninsula and China where the highest values are found. Chad and Mauritania stand out with 26.4% and 18.8%, respectively. Saudi Arabia and China present values of 16.7% and 16.1%, respectively. Extinction has a direct impact on solar resource assessment and thus on economic studies. Considering local atmospheric extinction values will result in more realistic LCOE values.

Keywords: Atmospheric Extinction, Atmospheric Attenuation, Solar radiation, Solar Spectral Irradiance, Solar Resource Assessment, Solar Tower Power Plants, LCOE, Concentrating Solar Power

1. Introduction

Solar radiation is attenuated as it passes through the Earth's atmosphere due to absorption and scattering processes resulting from the interaction with atmospheric constituents, such as aerosols and water vapour, among others. This phenomenon is known as atmospheric attenuation or atmospheric extinction. The amount of radiation attenuated by the atmosphere increases as the light path and the presence of atmospheric components do. Therefore, atmospheric attenuation maybe particularly strong for long distances in the lower layer of the atmosphere, where the density of these components, or their presence per unit volume, is higher.

Because of this, the solar radiation reflected by heliostats is partially extinguished on its path to the receivers in solar power tower plants (Barbero et al., 2021). A solar power tower plant basically consists of three subsystems: a heliostat field, a receiver, and a tower. The heliostat field is a set of mirrors, called heliostats, which follow the movement of the sun to reflect the solar direct normal irradiance (DNI) onto the receiver at the top of the tower. The receiver absorbs the solar radiation collected by the heliostat field and converts it into process heat at high temperatures. This heat is converted into electricity in the same way as conventional power plants.

Until now, DNI has been considered the key parameter for site selection and design of solar power tower plants. However, atmospheric attenuation limits the amount of local solar resource that can be exploited in solar power tower plants, so that the plant power output is reduced compared to what is expected. This is most noticeable in large plants and when the local climate is heavily loaded with atmospheric aerosols, such as in arid or desert regions. A reduction in solar plant power output can delay the economic recovery of the initial investment for the implementation of solar tower projects, which can lead to project failure.

In a recent study, Marzo et al. (Marzo et al., 2021) have shown that atmospheric extinction plays an important role not only in this phase of solar power tower projects, but also in their economic evaluation (see fig. 1). In their paper, they propose to introduce the atmospheric extinction parameter into the equation for calculating the LCOE(t) for solar power tower plants. By performing a sensitivity analysis of the proposed equation, they calculate the impact of this parameter on the final value of LCOE(t). The result is that the atmospheric extinction parameter can have a high

Selection and/or peer review under responsibility of Scientific Committee
doi:10.18086/swc.2021.37.05 Available at http://proceedings.ises.org

impact on the LCOE(t) value at locations with an atmospheric extinction of more than 10%.

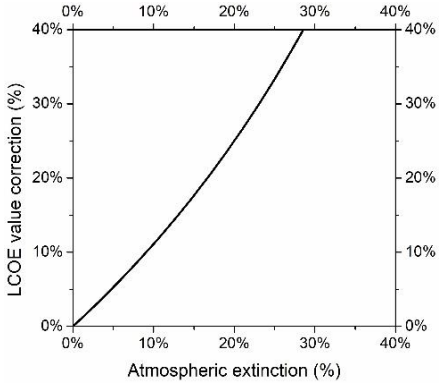

Fig. 1 Correction to be applied to the levelized cost of energy (LCOE) values if energy losses in solar tower power plants due to atmospheric extinction are considered (Marzo et al., 2021) .

Numerous efforts have been made in the last decade to quantify, measure or estimate the atmospheric extinction in solar tower power tower. The methods developed to quantify atmospheric extinction can be classified as: direct measurement methods (Ballestrín et al., 2018, 2016; Goebel et al., 2011; Hanrieder et al., 2015; Sengupta and Wagner, 2012; Tahboub et al., 2012), indirect measurement methods (Barbero et al., 2021; Hanrieder et al., 2012; Navarro et al., 2016) and model estimation methods (Alonso-Montesinos et al., 2020; Ballestrín et al., 2020; Cardemil et al., 2013; Carra et al., n.d.; Hanrieder et al., 2020; Marzo et al., 2021; Mishra et al., 2020; Polo et al., 2016).

Among the direct methods, the CIEMAT-system (Ballestrín et al., 2018) stands out because it has been operating for more than 4 years without failures at Plataforma Solar de Almería (PSA), Spain. CIEMAT-system is based on simultaneous measurements of the grey levels of images of a Lambertian target taken with two cameras 742 m apart. The relevant image processing allows the calculation of the atmospheric transmittance between the two cameras and, consequently, to obtain the extinction values. CIEMAT-system has enabled the development and validation of atmospheric extinction models (Alonso-Montesinos et al., 2020; Ballestrín et al., 2020; Carra et al., n.d.; Marzo et al., 2021; Polo et al., 2016). One of the validated models is the one used to make the world's first atmospheric extinction map, with application to solar tower power plants located in Chile (Marzo et al., 2021).

For the mapping, Marzo et al. developed a methodology based on the analysis of 30 years of historical MERRA-2 atmospheric parameter data at each location. After appropriate data processing, Marzo et al. were able to calculate the solar spectrum at different heights using the LibRadTran radiation transfer code (Emde et al., 2016; Mayer et al., 2020). With this information, the spectral extinction coefficient was obtained for the atmospheric layer of interest. By applying the Lambert-Beer-Bouguer's law, the transmittance and atmospheric extinction were obtained for the different slant ranges found in a 115 MW solar power tower plant, more information in (Marzo et al., 2021).

In this paper we show preliminary results of the application of this methodology to the assessment of heliostat-to-tower atmospheric extinction in solar tower power plants along the Sun Belt.

2. Materials and methods

The present paper applies the same methodology as the one described in (Marzo et al., 2021). This methodology was validated with the CIEMAT-system at the PSA, Spain, as reported in said reference. This time, the results show the atmospheric extinction for slant ranges of one kilometer considering a 150 m high tower at 14 locations along the Sun Belt. One kilometer and 150 m high is the average heliostat-to-tower distance and the average tower height in a 115 MW power plant, which is a representative power output of today's solar tower power plants.

For the analysis, the Modern-Era Retrospective Analysis for Research and Applications, version 2, also called MERRA-2 (Gelaro et al., 2017), was consulted. MERRA-2 is an atmospheric reanalysis of the Era satellite produced by NASA's Global Modelling and Assimilation Office (GMAO). The model uses a grid resolution of 0.5° latitude and 0.625° longitude. MERRA-2 includes the assembly of aerosol data, providing a reanalysis in which aerosols and meteorological observations are assembled in a global data assembly system.

To have a large representative sample of the atmospheric parameters at each location, MERRA-2 data from the last 30 years, from January 1989 to December 2018, were analyzed for all points studied within the Sun Belt.

The analyzed database includes not only the parameters of interest for the topic of atmospheric extinction, but also those that may be related with atmospheric radiative transmittance and the shape of the solar spectrum: atmospheric pressure at ground level [Pa], relative humidity [%], atmospheric pressure at sea level [Pa], temperature at 2 m [K], ozone [Dobson], precipitable water [kg m^{-2}], Ångström parameter [470, 870] nm, total aerosol extinction, aerosol optical thickness (AOT) at 550 nm (τ550), scattering coefficient of aerosols at 550 nm. The collection of all these data corresponds to step 1 of the methodology diagram in Fig. 2.

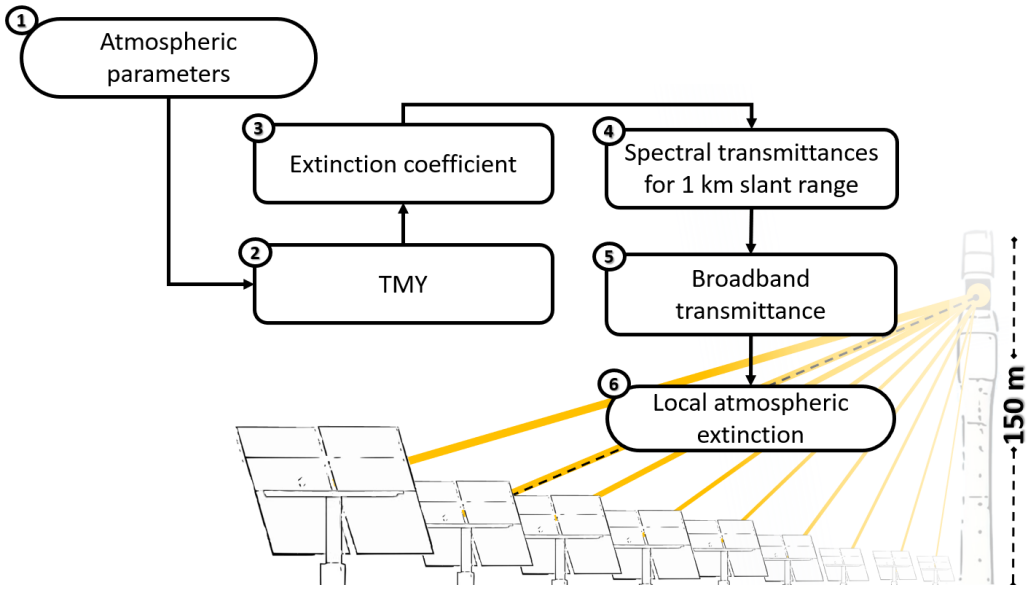

Fig. 2 Diagram summarizing the methodology used to estimate the local atmospheric extinction for 1 km slant range. This figure graphically simulates how the extinction affects the radiation, light, travelling through the atmosphere, decreasing the visibility of distant objects, in this case the tower from the observer's point of view, as its effect increases with the distance travelled by the light.

Subsequently, step 2 refers to the data processing to calculate the typical meteorological year (TMY) according to the methodology described in (Wilcox and Marion, 2008).

Once the TMY was calculated, LibRadTran was used to calculate the spectral transmittance values of the vertical column of atmosphere, $T^v_{\lambda\_h}$, from the outer layer to the considered height h, at each location and time of TMY. In this case, the altitudes considered for the study were 0 m, ground level, and 150m height, corresponding to the atmospheric transmittances from the outer layer to 0 m ($T^v_{\lambda\_0m}$) and 150 m ($T^v_{\lambda\_150m}$). LibRadTran allows the vertical variability of atmospheric properties to be included. For this purpose, the atmosphere is divided into a series of homogeneous layers, characterized by different optical thicknesses, phase function and single scattering albedo (Marzo et al., 2021). In this paper, the atmosphere defined in the US-standard LibRadTran file was used as input to define the vertical properties of the atmosphere. For the distribution of the aerosol characteristics with height, the aerosol_profile_modtran file was used as input, which linearly distributes the aerosol characteristics up to 6 km (as in the ModTran software) when altitude is non-zero. For a more detailed description of how these files do the distribution of atmospheric properties with height, please refer to (Emde et al., 2016; Mayer et al., 2020).

An intermediate step is multiplying $T^v_{\lambda\_0m}$ by the extra-terrestrial spectrum it is possible to obtain the spectral direct normal irradiance (DNI_λ) at each time of the TMY, which corresponds to an estimate of the solar resource reaching the heliostat under clear sky conditions. This data is reserved for a later step.

From the Lambert-Beer-Bouguer law and the information provided by both spectra, the spectral extinction coefficient for the atmospheric layer between 0 and 150 m was obtained as follows, for further details see (Marzo et al., 2021):

$$\kappa_{\lambda\_150\mathrm{m}} = -\ln\left(\frac{T^v_{\lambda\_0m}}{T^v_{\lambda\_150m}} * \frac{1}{h}\right) \qquad \text{(eq. 1)}$$

where κ_{λ_150m} is the average spectral extinction coefficient, for the atmospheric layer between 0 and 150 m.

Once the spectral extinction coefficient has been calculated, it is possible to calculate the spectral transmittance for 1 km distance, $T_\lambda(1km)$, under the local atmospheric conditions described for the calculation of the solar spectra at 0 and 150 m, by using Lambert-Beer-Bouguer's law.

$$T_\lambda(1km) = \frac{I_{\lambda\_2}}{I_{\lambda\_1}} = e^{-\kappa_\lambda s} \quad \text{(eq. 2)}$$

Now, it is possible to multiply $T_\lambda(1km)$ by the DNI_λ at that time of the TMY and the heliostat spectral reflectance, ρ_λ, giving the amount of radiation reaching the receiver. Subsequently, the broadband value is calculated, as follows, and averaged for the whole year resulting in an annual mean value of the 1 km slant range transmittance of the place.

$$T(1km) = \frac{\int_{300}^{2500} T_\lambda(1km)\, \rho_\lambda\, DNI_\lambda\, d\lambda}{\int_{300}^{2500} \rho_\lambda\, DNI_\lambda\, d\lambda} \quad \text{(eq. 3)}$$

The average value of the annual atmospheric attenuation for a 1 km slant range, $A(1km)$, is obtained from its definition as follows:

$$A(1km) = 1 - T(1km) \quad \text{(eq. 4)}$$

For more details and other related calculations see (Marzo et al., 2021).

3. Results

Solar irradiation is a crucial parameter in solar power plant projects using tower technology. This parameter is useful for site selection, solar power plant design and has a great impact on economic studies, such as the levelized cost of electricity (LCOE). However, as explained above, normal direct solar irradiation can be partially extinguished in the heliostat-to-tower path. For this reason, it is inappropriate to evaluate only the direct normal irradiation without considering the atmospheric extinction for the assessment of the solar resource in the framework of solar power tower plants. There is not much information on atmospheric extinction values around the world, except for the locations shown in some specific studies. To get a more global view of atmospheric extinction values, 14 locations around the world were selected.

Figure 3 shows the location of the Sun Belt sites that have been analyzed in this paper. All selected sites are in the Sun Belt. The Sun Belt is the area where the greatest amount of solar radiation is received throughout the year on the Earth. It comprises two bands that encircle the planet. It is located around the tropics of Cancer and Capricorn north and south of the equator. It is in the Sun Belt that most of the world's deserts are located, apart from Antarctica and the Arctic.

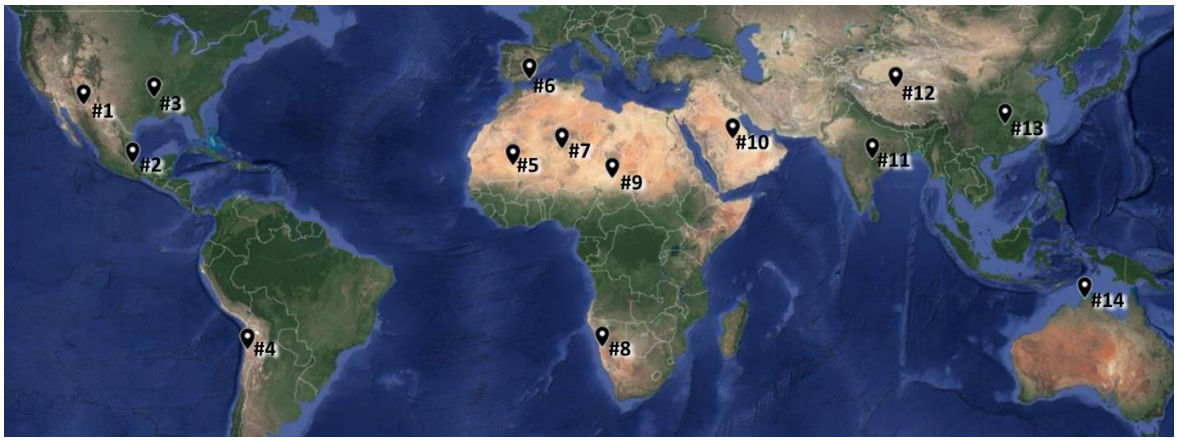

Fig. 3 Analyzed locations along the Sun Belt (source: Google Maps).

The high availability of solar resources and the extreme atmospheric conditions of desert environments make the sunbelt an area of interest for analysis in this paper.

The results of the atmospheric extinction calculations for 1 km slant range are shown in table 1. The colour scale indicates the distribution of extinction values, where green indicates the lowest values and red the highest. These values are obtained by applying the methodology described above. Table 1 also shows geographical and climatic information on the sites considered, as well as their elevation from sea level.

Table 1: Results of the annual average of atmospheric extinction values for a 1 km slant range for the analyzed locations

N°	Latitude	Longitude	Country	Köppen-Geiger Climate Classification*	Elevation (m)	Atmospheric extinction for 1km slant range
#1	32.00	-109.38	USA	BSk	1672	5.1%
#2	19.50	-97.50	Mexico	Cfb	2552	5.9%
#3	33.50	-92.50	USA	Cfa	47	7.3%
#4	-24.09	-69.93	Chile	BWk	965	4.0%
#5	19.00	-6.25	Mauritania	BWh	327	18.8%
#6	37.09	-2.36	Spain	BSk	490	6.6%
#7	22.79	5.53	Argelia	BWh	1380	11.1%
#8	-23.56	15.04	Namibia	BWh	409	6.4%
#9	16.00	17.50	Chad	BWh	385	26.4%
#10	24.91	46.41	Saudi Arabia	BWh	755	16.7%
#11	20.50	80.00	India	Aw	226	11.2%
#12	35.50	85.62	China (Tibet)	ET	5254	4.9%
#13	28.00	111.87	China	Cfa	636	16.1%
#14	-12.42	130.89	Australia	Aw	34	8.3%

* *source* (Kottek et al., 2006). ***Main climates:*** *A, equatorial; B, arid; C,warm temperate; D, cold continental; E, polar.* ***Precipitation:*** *W, desert; S,steppe; f, fully humid; s, summer dry; w, winter dry, m, monsoonal.* ***Temperature:*** *h, hot arid, low latitude; k, cold arid, middle latitude; a, hotsummer; b, warm summer; c, cold summer.*

The annual extinction values for the sites considered are between 4.0% and 26.4%, corresponding to Chile and Chad, respectively. In other words, the local lower atmosphere causes annual energy losses in solar power tower plants with values between 4% and 26% depending on the place. In general, it can be concluded that atmospheric extinction represents an average of 10.6% of energy losses per year for the stations considered in the study.

The highest annual average values of atmospheric extinction correspond to locations in Mauritania and Chad with 18.8% and 26.4%, respectively. In general, high values (>10%) are found mainly in arid and desert climates (BW), as well as in China (Cfa) and India (Aw). Within arid and desert climates (BW) climates, Chile and Namibia stand out for their low extinction values, 4.0% and 6.4%, respectively.

From these preliminary results, there does not seem to be a relationship between atmospheric extinction and climate type. Thus, for example, it is possible to find the highest and lowest levels of extinction in desert climates (BW), such as in Chad and Chile.

However, it is observed that the highest extinction values coincide with areas where atmospheric aerosol content is high. For example, the Sahara Desert in West Africa, known for its high aerosol content in episodes such as calima, has annual extinction values above 11% in Algeria (BWh), 18.8% in Mauritania (BWh), and 26.4% in Chad (BWh).

High values of aerosol content, linked to anthropogenic factors (Filonchyk et al., 2019), are also found in China and India resulting in extinction values of 16.1% and 11.2%, respectively.

Among the places analyzed, Chile stands out with an extinction value of 4.0% for the Plataforma Solar del Desierto de Atacama (PSDA) at 965 m.a.s.l., and China with a value of 4.9% at 5254 m.a.s.l. near the Tibet region.

Regardless of the magnitude of the extinction values found, it is important to consider atmospheric extinction in the planning and design of solar tower power plants and in economic studies, such as LCOE.

The results shown in this paper cannot be extrapolated to other locations in the country under consideration. They are only taken as an example to show the importance that atmospheric extinction can have in the evaluation of the solar resource in the context of solar power tower plants. To obtain results applicable to different national territories, more in-depth studies, such as the one carried out in (Marzo et al., 2021), should be considered.

However, the results already indicate that the annual DNI value might be insufficient for the assessment of solar tower projects in some locations. Not considering atmospheric extinction losses may lead to an overestimation of solar resource availability and incorrect conclusions in studies related to solar power tower plants.

4. Conclusions

The solar radiation collected by heliostats in solar power tower plants can be partially extinguished depending on the content of atmospheric components and the distance travelled to the receivers on the towers. Atmospheric extinction is a difficult issue to quantify or estimate, which has been studied in the last decade due to the growing concern of the solar industry and investors about the lack of information on the subject.

This paper presents preliminary results of the evaluation of heliostat-to-tower atmospheric extinction values for a 1 km slant range in places sited along the Sun Belt.

The methodology employed is based on the use of long-term model retrieval databases, the LibRadtran radiative transfer code and the application of the Lambert-Beer-Bouguer law. This methodology has already been applied by the authors in a previous work for the elaboration of an atmospheric extinction map in Chilean territory and validated at the Plataforma Solar de Almería, Spain (Marzo et al., 2021) .

Overall, the results show that the extinction values are between 4% and 26% for 1000 m slant range for the sites analyzed.

High values (>10%) are found mainly in arid and desert climates. Thus, values of 19% are exceeded in West Africa, even reaching 26% in some places such as Chad. However, Chile stands out globally with values below 4% despite having a desert and arid climate.

These values of atmospheric extinction limit the amount of local useful solar resource available, which has a direct impact on the calculated LCOE values and puts the viability of solar tower power plant projects at risk.

5. Acknowledgments

The authors acknowledge the generous financial support provided by CORFO under the projects (Corporación de Fomento de la Producción) 17BPE3-83761, 13CEI2-21803, 16ENI2-71940 (ING2030) and 7PTECES-75830 under the framework of the project “AtaMoS TeC”, and the generous financial support provided by CONICYT under the project ANID/FONDAP/15110019 SERC-Chile. Authors also acknowledgment the financial support of the completed PRESOL project with references ENE2014-59454-C3-1-R1, 2 and 3 with ERDF funds. We are also grateful for the financial support from the Spanish Education and Competitivity Ministry, PVCastSoil project (references ENE2017-83790-C3-1,2,3) and co-financed by the European Regional Development Fund and the Spanish Ministry of Science and Innovation and co-financed by the European Regional Development Fund grant reference PID2020-118239RJ-I00 (MAPVSpain).

6. References

Alonso-Montesinos, J., Ballestrín, J., López, G., Carra, E., Polo, J., Marzo, A., Barbero, J., Batlles, F.J.J., Opez, G.L., Carra, E., Polo, J., Marzo, A., Barbero, J., Batlles, F.J.J., 2020. The use of ANN and conventional solar-plant meteorological variables to estimate atmospheric horizontal extinction. Journal of Cleaner Production 125395. https://doi.org/10.1016/j.jclepro.2020.125395

Ballestrín, J., Carra, E., Alonso-Montesinos, J., López, G., Polo, J., Marzo, A., Fernández-Reche, J., Barbero, J., Batlles, F.J., 2020. Modeling solar extinction using artificial neural networks. Application to solar tower plants. Energy 199, 117432. https://doi.org/10.1016/j.energy.2020.117432

Ballestrín, J., Monterreal, R., Carra, M.E., Fernandez-Reche, J., Barbero, J., Marzo, A., 2016. Measurement of solar extinction in tower plants with digital cameras, in: AIP Conference Proceedings. pp. 130002-1-130002–8. https://doi.org/10.1063/1.4949212

Ballestrín, J., Monterreal, R., Carra, M.E., Fernández-Reche, J., Polo, J., Enrique, R., Rodríguez, J., Casanova, M., Barbero, F.J., Alonso-Montesinos, J., López, G., Bosch, J.L., Batlles, F.J., Marzo, A., 2018. Solar extinction measurement system based on digital cameras. Application to solar tower plants. Renewable Energy 125, 648–654. https://doi.org/10.1016/j.renene.2018.03.004

Barbero, F.J., López, G., Ballestrín, J., Bosch, J.L., Alonso-Montesinos, J., Carra, M.E., Marzo, A., Polo, J., Fernández-Reche, J., Batlles, F.J., Enrique, R., 2021. Comparison and analysis of two measurement systems of horizontal atmospheric extinction of solar radiation. Atmospheric Environment 118608. https://doi.org/10.1016/j.atmosenv.2021.118608

Cardemil, J.M., Starke, A.R., Scariot, V.K., Grams, I.L., Colle, S., 2013. Evaluating solar radiation attenuation models to assess the effects of climate and geographical location on the heliostat field efficiency in Brazil, in: Energy Procedia 49, 1288-1297. https://doi.org/10.1016/j.egypro.2014.03.138

Carra, E., Marzo, A., Ballestrín, J., Polo, J., Barbero, J., Alonso-Montesinos, J., Monterreal, R., Abreu, E.F.M.E.F.M., Fernández-Reche, J., n.d. Atmospheric extinction levels of solar radiation using aerosol

optical thickness satellite data. Validation methodology with measurement system. Renewable Energy 149, 1120–1132. https://doi.org/10.1016/j.renene.2019.10.106

Emde, C., Buras-Schnell, R., Kylling, A., Mayer, B., Gasteiger, J., Hamann, U., Kylling, J., Richter, B., Pause, C., Dowling, T., Bugliaro, L., 2016. The libRadtran software package for radiative transfer calculations (version 2.0.1). Geoscientific Model Development 9, 1647–1672. https://doi.org/10.5194/GMD-9-1647-2016

Filonchyk, M., Yan, H., Zhang, Z., Yang, S., Li, W., Li, Y., 2019. Combined use of satellite and surface observations to study aerosol optical depth in different regions of China. Scientific Reports 2019 9:1 9, 1–15. https://doi.org/10.1038/s41598-019-42466-6

Gelaro, R., McCarty, W., Suárez, M.J., Todling, R., Molod, A., Takacs, L., Randles, C.A., Darmenov, A., Bosilovich, M.G., Reichle, R., Wargan, K., Coy, L., Cullather, R., Draper, C., Akella, S., Buchard, V., Conaty, A., da Silva, A.M., Gu, W., Kim, G.K., Koster, R., Lucchesi, R., Merkova, D., Nielsen, J.E., Partyka, G., Pawson, S., Putman, W., Rienecker, M., Schubert, S.D., Sienkiewicz, M., Zhao, B., 2017. The modern-era retrospective analysis for research and applications, version 2 (MERRA-2). Journal of Climate 30, 5419–5454. https://doi.org/10.1175/JCLI-D-16-0758.1

Goebel, O., Luque, F., Alobaidli, A., Salbidegoitia, I., 2011. Beam Attenuation Test for Central Tower Power Plants in a High Density Aerosol Atmosphere – Setup & Methodlogy SolarPACES 2011. Proceedings of Solar Power and Chemical Energy Systems conference (SolarPACES 2011) 8-16.

Hanrieder, N., Ghennioui, A., Wilbert, S., Sengupta, M., Zarzalejo, L.F., 2020. AATTENUATION-The Atmospheric Attenuation Model for CSP Tower Plants: A Look-Up Table for Operational Implementation. Energies 13, 5248. https://doi.org/10.3390/en13205248

Hanrieder, N., Wehringer, F., Wilbert, S., Wolfertstetter, F., Pitz-Paal, R., Campos, V.Q., Quaschning, V., Campos, A., Quaschning, V., 2012. Determination of Beam Attenuation in Tower Plants. SolarPACES 11, 2012.

Hanrieder, N., Wilbert, S., Pitz-Paal, R., Emde, C., Gasteiger, J., Mayer, B., Polo, J., 2015. Atmospheric extinction in solar tower plants: absorption and broadband correction for MOR measurements. Atmospheric Measurement Techniques 8, 3467–3480. https://doi.org/10.5194/amt-8-3467-2015

Kottek, M., Grieser, J., Beck, C., Rudolf, B., Rubel, F., 2006. World Map of the Köppen-Geiger climate classification updated. Meteorologische Zeitschrift 259–263. https://doi.org/10.1127/0941-2948/2006/0130

Marzo, A., Salmon, A., Polo, J., Ballestrín, J., Soto, G., Quiñones, G., Alonso-Montesinos, J., Carra, E., Ibarra, M., Cardemil, J., Fuentealba, E., Escobar, R., 2021. Solar extinction map in Chile for applications in solar power tower plants, comparison with other places from sunbelt and impact on LCOE. Renewable Energy 170, 197–211. https://doi.org/10.1016/j.renene.2021.01.126

Mayer, B., Kylling, A., Emde, C., Buras, R., Hamann, U., Gasteiger, J., Richter, B., 2020. libRadtran user's guide.

Mishra, B.R., Hanrieder, N., Modi, A., Kedare, S.B., 2020. Comparison of three models to estimate the slant path atmospheric attenuation in central receiver solar thermal plants under Indian climatic conditions. Solar Energy 211, 1042–1052. https://doi.org/10.1016/j.solener.2020.10.049

Navarro, A.A., Ramírez, L., Domínguez, P., Blanco, M., Polo, J., Zarza, E., 2016. Review and validation of Solar Thermal Electricity potential methodologies. Energy Conversion and Management 126, 42–50. https://doi.org/10.1016/j.enconman.2016.07.070

Polo, J., Ballestrín, J., Carra, E., 2016. Sensitivity study for modelling atmospheric attenuation of solar radiation with radiative transfer models and the impact in solar tower plant production. Solar Energy 134, 219–227.

Sengupta, M., Wagner, M., 2012. Atmospheric attenuation in central receiver systems from dni measurements. Proceedings of Solar Power and Chemical Energy Systems conference (SolarPACES 2012) 6. https://doi.org/10.1115/ES2012-91229

Tahboub, Z.M., Aziz, A., Obaidli, A., Luque, F., Salbidegoitia, I., Farges, O., Oumbe, A., Geuder, N., Goebel, O., 2012. Solar Beam Attenuation Experiments – Abu Dhabi. SolarPaces Conference.

Wilcox, S., Marion, W., 2008. Users Manual for TMY3 Data Sets. Golden, Colorado .